



Methodology for processing backscattered electron images. Application to Aguada archaeological paints

V.Galván Josa^a, S.R. Bertolino^{a,b}, J.A. Riveros^{a,b}, G. Castellano^{a,b,*}

^aFaMAF, Universidad Nacional de Córdoba, Medina Allende s/n, Ciudad Universitaria, (5016) Córdoba, Argentina

^bCONICET, Argentina

ARTICLE INFO

Article history:

Received 30 May 2009

Received in revised form 6 July 2009

Accepted 6 July 2009

Keywords:

SEM

Backscattered electron images

Image processing

XRD

Paint characterization

Elemental analysis

Aguada culture

ABSTRACT

Scanning electron microscopy is a powerful technique in several fields of science and technology. In particular it is an important complement in the characterization of materials for which X-ray analysis is not possible. Such is the case of thin paint layers on ceramic pots, in which, even for low incident energies, the electron interaction volume can be greater than the paint thickness—in addition to the problem arising from similar compositions. With the aim of complementing other common techniques used in compositional materials characterization, in this work, an image-processing software has been developed, which implements a new methodology for the treatment of backscattered electron (BSE) images in order to bring to evidence small mean atomic number contrasts, usually imperceptible to human eye. The program was used to study black and white pigments of ceramic pieces belonging to the Ambato style of “Aguada” culture (Catamarca province, Argentina, IV–XII centuries AD). Although the BSE images acquired for these samples showed no apparent contrast between sherd and black and white pigments, through image-processing algorithms using different space filters, chemical contrast between regions has been brought to evidence with a minor detail loss. This has been accomplished by applying a smoothing filter, after which the main routine for contrast enhancement reveals details in the grey-level region of interest; finally, a filter for edge enhancement permits to recover some details lost in the previous steps, achieving satisfactory results for the painted sherd samples analyzed. In order to validate the mean atomic number differences found between each pigment and the ceramic body, X-ray diffraction diagrams have been refined with Rietveld method using the software DIFFRACplus Topas[®], arriving to mineralogical differences which agree with the results obtained. As a consequence of this study, the program developed has proven to be a suitable tool for routine analysis of samples with slight chemical contrast.

© 2009 Elsevier Ltd. All rights reserved.

1. Introduction

X-ray analytical techniques, such as X-ray fluorescence (XRF), total reflection X-ray fluorescence (TXRF), X-ray diffraction (XRD) and scanning electron microscopy complemented with energy dispersive X-ray spectrometers (SEM-EDX), are valuable tools for surface characterization which have widely been used for the analysis of archaeological pieces (Aloupi et al., 2000; Barrios Neira et al., 2009; Buxeda i Garrigós, 1999; Cariati et al., 2003; Fernández-Ruiz and García-Heras, 2007; Fortina et al., 2008; Iordanidis et al., 2009; Mirti, 2000; Schleicher et al., 2008; Schreiner et al., 2004). The popularity of these techniques lies

not only in their non-destructive character and relatively low-cost analyses, but also in the fact that the simultaneous application of them allows mineralogical (XRD) and chemical (XRF, TXRF and SEM-EDX) analysis of decorated sherds (Appolonia et al., 2001; Craig et al., 2007). An alternative for studying sherd surfaces finished with clay coatings or colour paints is to scrap a small amount of material (≈ 10 mg), in order to perform the analysis independently of the ceramic body. Laser ablation-inductively coupled plasma-mass spectrometry (LA-ICP-MS) (Bao-Ping et al., 2005; Cochrane and Neff, 2006; Papadopoulou et al., 2004; Pérez-Arantegui et al., 2008) and neutron activation analysis (NAA) are techniques also used for chemical characterization, and permit a concentration detection of a few parts per billion (ppb = ng/g) in micrograms of sample (Habicht-Mauche et al., 2002; Neff, 2003; Speakman and Neff, 2002; Vaughn et al., 2006); however, they present the disadvantage of high-cost analysis and limited availability of nuclear reactor centers in the case of neutron activation (Odell, 2006; Papadopoulou et al., 2004; Pérez-Arantegui et al., 2008). Also Mössbauer spectroscopy is commonly

* Corresponding author at: FaMAF, Universidad Nacional de Córdoba, Medina Allende s/n, Ciudad Universitaria, (5016) Córdoba, Argentina.
Tel.: +54 351 4334051; fax +54 351 4334054.

E-mail address: gcas@famaf.unc.edu.ar (G. Castellano).

used for determining iron oxidation states in archaeological samples (Molera et al., 1998), an important issue when studying the colour origin. Alternatively, Raman spectroscopy is a complementary technique, one of its main applications on the archaeology and art history being pigment identification (Smith and Clark, 2004). Usually paint layers contain metallic oxides or sulfates, which allows to elaborate paint and pigment catalogs, although several problems may arise depending on the excitation source energy (Edwards and Chalmers, 2005).

Similarly, in an electron microscope, Auger and backscattered electron signals are generated in regions close to the sample surface, complementing the X-ray spectral information (Goldstein et al., 1992; Polak et al., 1983). Although Auger spectroscopy may provide accurate analysis, several experimental difficulties, in addition to the expensive character of the involved instruments, inhibit a frequent use of this technique. On the other hand, backscattered electron (BSE) images may provide certain chemical-contrast information from the surface of the studied material, since the fraction of backscattered electrons increases with the mean atomic number Z of the irradiated sample (Reed, 1993). For this reason, BSE images constitute an attractive alternative to this aim, since backscattered electrons are mainly emitted from an intermediate zone close to the surface and allow the distinction of small variations ΔZ in the mean atomic number: in very low noise BSE images, a discrimination eventually up to $\Delta Z \approx 0.1$ (Goldstein et al., 1992) may be achieved.

When two regions of a sample present slight chemical contrast (i.e., similar mean atomic numbers), 8-bit BSE signal grey levels will also be similar. In this case, simple human eye recognition in BSE images becomes difficult in view of our limited 30 grey-level discrimination power (Russ, 1998). Although this is a relevant question for surface characterization through BSE imaging, the problem has scarcely been faced in the literature, and only morphological developments have been done in this area (Chinga-Carrasco et al., 2009; Tzaphlidou, 2005).

For these reasons, a methodology for image processing has been developed in this work, in order to allow the maximum profit of the information contained in these images, with the capability of distinguishing between similar mean atomic number regions. The methodology proposed here consists in the application of several filters, intended to subtract noise and fluctuations which are inherent to the measurement process (Gonzalez and Woods, 2002; Russ, 1998). With this kind of procedure, pixels are not considered as isolated points, but global trends in the image are taken into account instead. After a smoothing process, in order to discriminate close grey levels, contrast is enhanced in the region of interest, which always implies certain detail loss. Finally, the program developed permits an edge-enhancement procedure, allowing the identification of each pigment region.

Scanning electron microscopy (SEM) combined with X-ray diffraction (XRD) have extensively been used for studying archaeological pieces and pigments (Bertolino and Fabra, 2003; De La Fuente et al., 2005; De La Fuente, 2006; Druc, 2001). The fact that only small amounts of archaeological samples are available has increasingly encouraged the application of these techniques in this area during the last decades (Reed, 1993; Sánchez Ramos et al., 2002). The analysis of pottery paints and pigments is a major quest not only in archaeology, but also in Art History, since the understanding of deterioration processes and conservation methods are necessary for distinguishing original parts from subsequent amendments, ulterior restoration works or counterfeits. In this work the methodology proposed has been applied to characterize pigments used in pottery fabrication of the Ambato style of "Aguada" culture (Catamarca province, Argentina), which, according to different studies, has flourished from IV to XII centuries AD (Baldini et al., 2002; Laguens and Bonnin, 2005; Pantorrilla and

Núñez Regueiro, 2006). Such analysis has not been completed up to now, and only qualitative analyses can be found in the literature (Bertolino and Fabra, 2003; De La Fuente et al., 2005; De La Fuente, 2006). This is an important application of this approach, since this characterization will complement previous studies in this area (Bertolino et al., 2009).

It must be mentioned that energy dispersive X-ray (EDX) analysis is not suitable for this kind of samples. EDX spectral characteristic lines are built-up through ionizations occurred in all the interaction volume covered by the primary beam, whose typical dimensions may reach $5 \mu\text{m}$ under normal operating conditions. This becomes a strong limitation when thin paint layers are to be analyzed, since their thickness is not always homogeneous and their surface is quite uneven. Anyway, EDX spectra are very useful for the identification of major and minor elements present in each phase, though this is almost impossible with trace elements, since signal-to-noise ratio inhibits their detection. Similarly, by increasing the incident electron beam energy, the penetration depth increases, which allows to ionize deeper regions: important changes in the set of elements identified in the registered spectrum permit to infer if multiple paint layers have been applied.

2. Implementation of BSE image-processing routines

In order to make mean atomic number contrast more evident, circumscribe regions corresponding to each pigment, improve focus and reduce noise due to roughness, BSE images must be processed. Specific transformations have to be applied, modifying each pixel grey level according to its value and those of its neighbour pixels—not to its location. These functions are usually called filters (Russ, 1998), and its implementation is based on a convolution mechanism. Convolution filters can be represented by a rectangular $M \times N$ matrix, which is moved across the image so that its central element coincides with each image pixel. In each position, every pixel value is multiplied by the corresponding element of the convolution matrix. Finally, the central matrix element is replaced by this product sum. Some kind of test is necessary in order to determine which routines are more suitable for each case.

Different transformations have been implemented in the program developed in this work. The processing routine followed for the application chosen here basically consists of three steps:

2.1. Smoothing

These methods are pixel-to-pixel operations intended to reduce noise as well as contrast between neighbouring pixels (Russ, 1998). Since details are associated not with single pixels, but with the structure surrounding every location, it is important to bear in mind that any smoothing operation implies a loss of information. This means that no general criterion can be established for the best smoothing procedure. It must be noticed that certain filters may introduce undesirable noise, as is the case of the well-known Savitzky–Golay filter (Savitzky and Golay, 1964), which is inappropriate when dealing with sharp edges. The smoothing algorithms tested in the program developed involve low-pass filters (Bonnet, 2004).

2.2. Contrast enhancement

The transformation written with the aim of exaggerating the contrast between regions which must be discriminated consists in stretching the grey-level scale in the range of interest (Chen and Ramli, 2003; Jafar and Ying, 2008). The function $T(i, j)$ which

produces a new image covering most of the grey-level scale can be defined as

$$T(i, j) = \begin{cases} b(i, j)v_1/u_1 & \text{if } b(i, j) \leq u_1 \\ [b(i, j) - u_1](v_2 - v_1)/(u_2 - u_1) + v_1 & \text{if } u_1 \leq b(i, j) \leq u_2 \\ [b(i, j) - u_2](255 - v_2)/(255 - u_2) + v_2 & \text{if } b(i, j) \geq u_2 \end{cases}$$

where u_1 and u_2 are the minimum and maximum grey levels of the region of interest, whereas v_1 and v_2 are the minimum and maximum grey levels desired, $b(i, j)$ is the smoothed image grey level in pixel (i, j) . The choice of u and v values strongly depends on the particular image studied. For the determination of u_1 and u_2 , the program permits the selection of a rectangular window of arbitrary size in order to obtain the average grey level inside it.

The disadvantage of this step is the saturation of the image and partial loss of information outside the regions of interest. However, those slight differences in chemical contrast, originally hidden to human eye, are brought to evidence, which is the purpose of this particular step.

2.3. Edge enhancement

Transitions from a region to another with a different grey level may denote changes in composition. It is necessary to distinguish in the intensity fluctuations, those arising from surface imperfections or grain boundaries from those arising from compositional changes. Once the transformations detailed above have been applied, edges are poorly defined, since smoothing produces this blurring. Several algorithms have been developed for edge detection (Russ, 1998), most of them enhancing intensity changes, allowing the appropriate delimitation of each pigment zone. In this work, the enhancement of edges corresponding to compositional variations was performed by the application of Laplacian filters

(Neycenssac, 1993), which can be modified by the user in order to adequate it according to the particular case considered.

The implementation of these filters has been carried out by developing a program in MATLAB[®] environment. It presents a user-friendly graphic interface with drop-down menus and the possibility of working with several images simultaneously. It also allows studying details or specific image regions through a “zoom” tool. For phase analysis, the program allows to visualize line intensity profiles and to convert some grey levels to optional colors. At any stage, the program allows the use of several well-known transformations, as well as the implementation of any other filter designed by the user.

As described below, BSE images have successfully been processed with this software, which includes all the image transformations described above. These may be configured by means of different options, so that the best alternatives may be combined, according to the specific situation under study.

3. Experimental

3.1. Sample preparation

The analyzed Aguada pot sherd samples (Ambato Style) were found in Piedras Blancas archaeological site, Catamarca, Argentina. These typical roughly finished Aguada tricolour wares (Fabra, 2006; Laguens and Juez, 1999) (B7, B53, Fig. 1) correspond to large vessels used for beer storage and processing, which can be plain or decorated with human and fantastic motives painted in white, red and black. These vessels are related to an old technological tradition, which acquired a new meaning within the Aguada context.

Ultrasonic cleaning of the fragments chosen for SEM analysis was performed with the aim of removing contaminating powder remains. Samples were coated with carbon in order to ensure

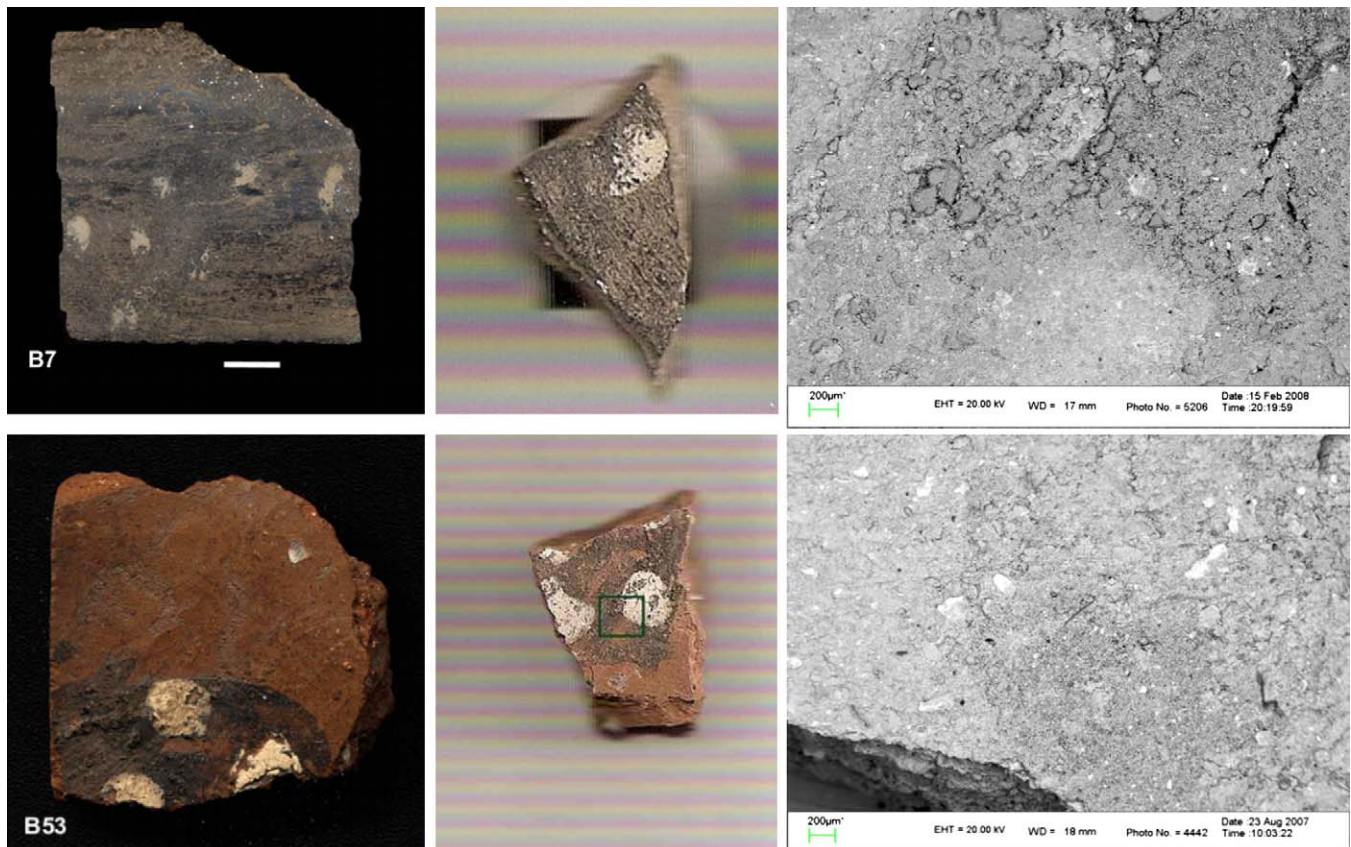


Fig. 1. Photographs and BSE images of sherds B7 and B53.

conductivity for irradiation in the SEM; this low atomic number coating was chosen because backscattered electrons are poorly attenuated (Goldstein et al., 1992).

A small amount of sample B53 was scraped from the surface and prepared in a random mount for XRD analysis. To this purpose, the samples were mounted on a low-background single-crystal Si holder, where small amounts of material (few milligrams) can be studied.

3.2. Data acquisition

Image acquisitions were carried out with a scanning electron microscope LEO 1450 VP, with an energy dispersive detection system attached. In order to acquire adequate BSE images, a scanning time large enough was selected, with the aim of minimizing statistical fluctuations, using a beam current of 300–400 pA and a 40 s scan frame time. Examples of such images are displayed in Fig. 1. Appropriate records were corroborated through linear profiles in BSE images collected at different acquisition times. Fig. 2 shows an example of such profiles, in which white lines represent the approximate mean fluctuation values for reddish and black paints respectively; their different heights reflect the differences in mean atomic numbers. These fluctuations

arise because the paint layer thickness is not homogeneous but rough and not plane, probably as a consequence of the burying of pieces for over 1000 years, being subjected to weathering and partial paint removal.

In order to validate the results obtained for chemical contrast through BSE imaging, mineral phases were characterized through X-ray diffraction. To this aim, random mounts of samples scraped from the surface of selected sherds were analyzed on a Philips X'Pert PRO PW 3040/60 diffractometer, using Cu K α X-ray radiation, Si monochromator, at 40 kV and 30 mA, step scan at 1°/100 s and step size of 0.02°, covering a 3–65° 2 θ range. Mineral phases present in the different pigments studied were quantified from the diffraction spectra through a Rietveld refinement procedure using the DiffracPlus TOPAS® - software (Bruker AXS, 2004). The method consists in fitting a theoretical model to an experimental XRD spectrum by the least squares method, in order to obtain the best fit between them (Young, 1993). The calculated diffraction pattern is based in a model that includes concentrations, structural parameters (spatial group, atom positions, thermal factors, etc.), microstructural parameters (crystal size, microdeformations) and instrumental parameters (instrumental contribution to the FWHM and peak shape, penetration of the incident beam on the sample, etc.). Background was fitted with a simple 6 degree polynomial function. Overall atomic displacement factors were used for each structure. The individual isotropic and anisotropic displacement factors for all phases were fixed. Positions and occupancy factors were refined for the major phases. For the peak description a PEARSON VII function was selected, which takes into account peak asymmetry corrections, and for the highly orientable phases (calcite, micas and feldspars) the March-Dollase correction model (Dollase, 1986; March, 1932) for preferred orientation was chosen. Values given in the Inorganic Crystal Structure Database (ICSD)¹ program were used as the starting parameters for the refinement.

4. Results and discussion

For an adequate image interpretation, the first step which must be performed is noise minimization. Depending on its nature, several methods can be chosen for its reduction (Gonzalez and Woods, 2002; Russ, 1998). In the case of the archaeological paints considered here, where noise originates in surface roughness, the optimal smoothing filter applied corresponds to a convolution matrix whose elements are all equal. Fig. 3 shows tests performed with different matrix sizes, demonstrating that for this case the most appropriate is a 3 × 3 matrix size, since a stronger smoothing procedure leads to severe detail and grain boundary losses.

After smoothing, it is necessary to enhance contrast between those grey levels which are to be discriminated. The function $T(i, j)$ defined to this aim in Section 2.2 is determined by the choice of the minimum and maximum grey levels of the region of interest, u_1 and u_2 , and the desired minimum and maximum grey levels, v_1 and v_2 . An example of this is shown in Fig. 4, where contrast is expected to be enhanced for the sample B7. In this case, a rectangular window containing pigments and naked sherd was selected, in order to obtain average grey levels inside it. The corresponding values resulted $u_1 = 175$ and $u_2 = 195$.

The last step in the implemented method consists in the enhancement of edges by means of the application of Laplacian filters, which have shown to be suitable for the images processed. Figs. 5 and 6 show the unprocessed images and those after the full image processing completing the three steps for sample B7 and B53, respectively.

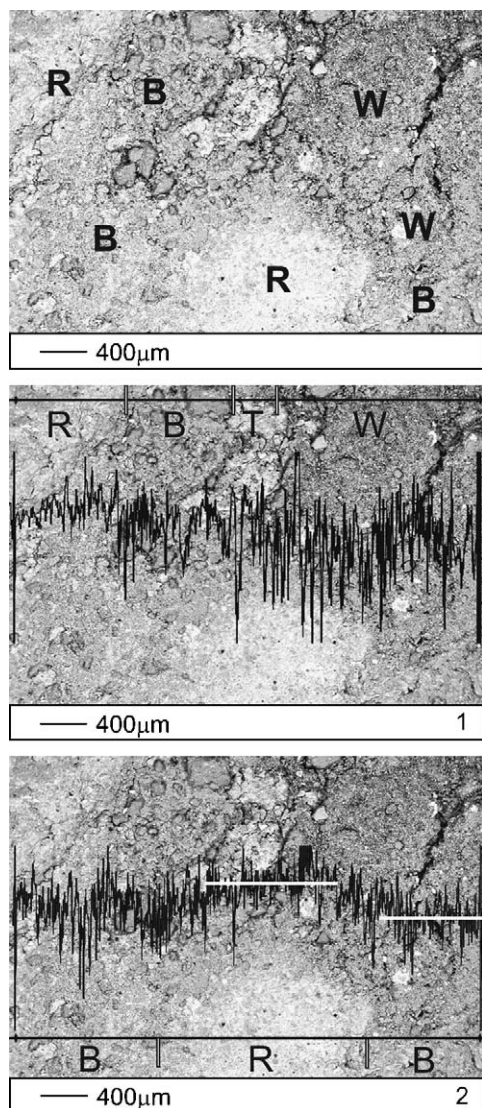


Fig. 2. B53 scan line profiles.

¹ <http://icsd.fiz-karlsruhe.de/icsd>.

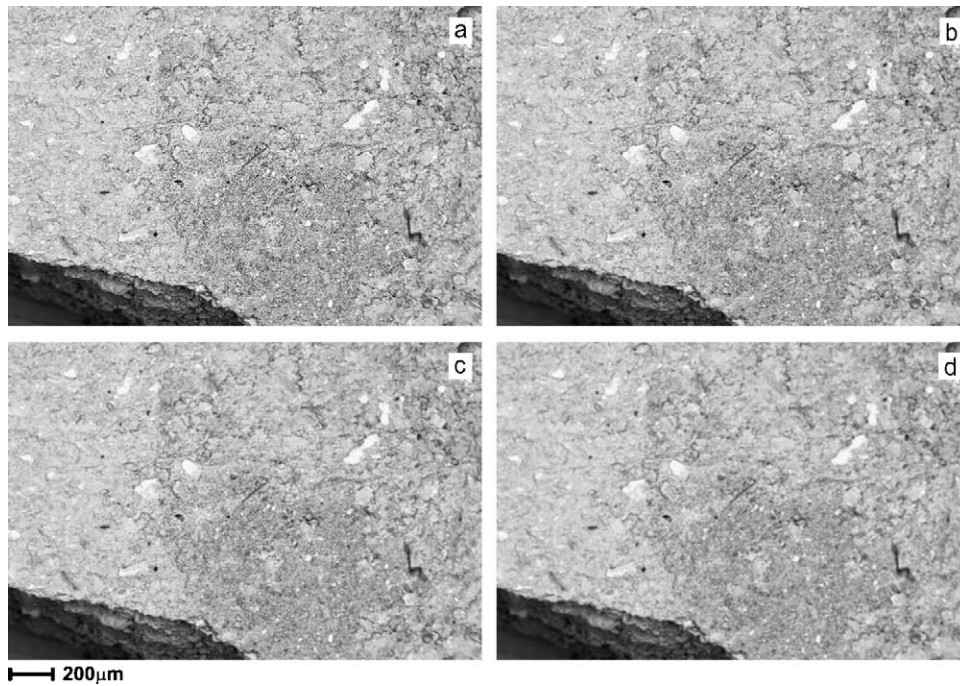


Fig. 3. Application of smoothing filters of different sizes in sample B7: (a) original image, (b) 3×3 , (c) 4×4 and (d) 5×5 .

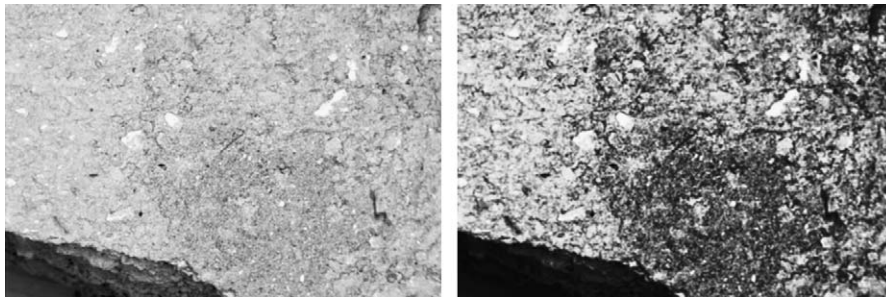


Fig. 4. B7 smoothed image (left) and image obtained after contrast enhancement $((u_1, u_2) \rightarrow (v_1, v_2))$.

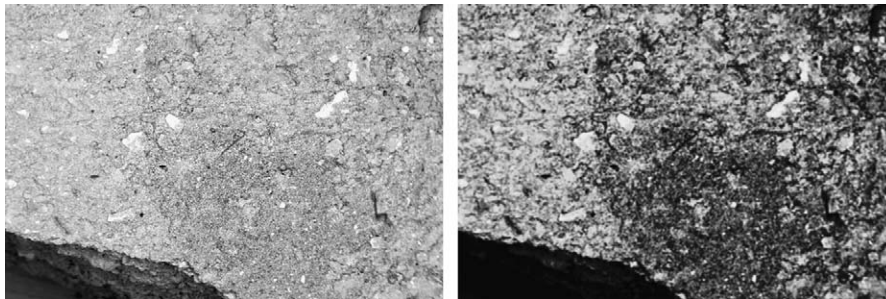


Fig. 5. Unprocessed (left) and optimized (right) BSE image for sample B7.

After BSE image processing has been completed for sample B7, it can be seen that regions corresponding to each pigment have satisfactorily been separated. Contrast between sherd and white and black paints has been emphasized, and the final transformation has led to an adequate edge enhancement. Some details can now be observed, not visible in the original image. Of course, the application of this transformations worsens the information outside the region of interest, but one can always return to the original image to start over with the process for every region of interest.

The BSE image contains no information to identify the elements present in the sample or their concentration levels. In order to

discard the possibility that the low chemical contrast observed does not originate from external contaminants, mineral phases were quantified by a Rietveld refinement procedure. Although in sample B7 the XRD analysis could not be performed due to lack of sufficient material, for sample B53 it was possible to scrap a sufficient amount of material as to acquire XRD patterns for the sherd surface. By means of a quantification procedure, mean atomic numbers were determined for white and black pigments, and for the ceramic pot.

Table 1 shows XRD quantification for white and black pigments and sherd for this sample. Structural formulae and ICSD numbers are also displayed. It can be seen that mean atomic number

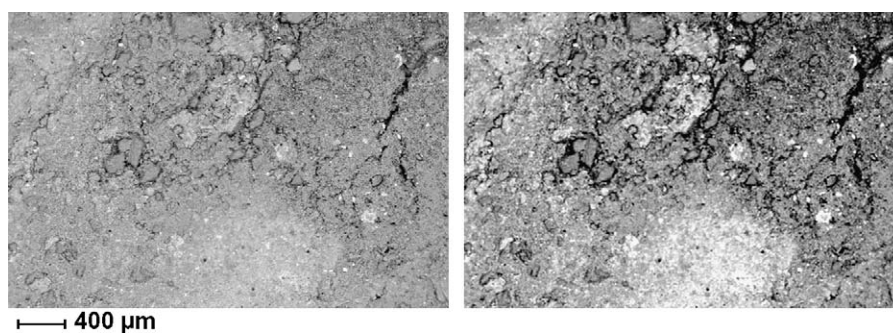


Fig. 6. Unprocessed (left) and optimized (right) BSE image for sample B53.

Table 1
XRD mineralogical characterization for B53 sherd and pigments.

Mineral	ICSD number	Structure	Mean Z	Sherd	Black	White
Quartz low	174	SiO ₂	10.0	27.0	50.3	54.8
Hematite	56372	Fe ₂ O ₃	15.2	≤0.5		
Muscovite	4368	KAl ₂ (AlSi ₃ O ₁₀)(OH) ₂	8.7	3.5	1.8	6.7
Hollandite	60787	Ba _{1.12} Al _{2.24} Ti _{5.76} O ₁₆	12.6		4.0	
Anorthite	86331	Ca(Al ₂ Si ₂ O ₈)	10.6	69.0	44.0	42.0
Hatchite	27304	PbTlAg(As ₂ S ₅)	45.0			≤0.5
Resulting mean Z in samples				10.40	10.37	10.34

differences result lesser than 0.1. However, it must be mentioned that diffraction patterns may reveal certain information from remainders of the ceramic body in the scraped paints, which might slightly mask greater differences in mean atomic numbers. Although this may systematically influence the results in this analysis, it must be kept in mind that the uncertainties caused by the Rietved refinement are negligible, and these results are quite reliable. Regarding the mineralogical characteristics of each region, white pigment of sample B53 owes its colour to the hatchite abundance in the translucent quartz and feldspar matrices, the reddish sherd colour corresponds to the presence of hematite, whereas the black pigment is characterized by its hollandite content. These are cases in which pigment characteristic colours are due to minority phases: for example, it is well known that even small proportions of lead mixed in a translucent media result in a good white pigment (Bertolino et al., 2009), as verified in the EDX spectrum identification of a weak Pb-M signal, as well as XRD characterization. This small amount of lead hardly influences the BSE signal, though this slight increase can be brought to evidence through an adequate image-processing method, as shown above.

In the right-hand side of Fig. 1, BSE images for the analyzed samples are displayed (B53 and B7). Both of them present low contrast and little detail can be appreciated.

The high quartz and feldspar contents both in pigments and sherd of sample B53 inhibit to obtain a good chemical contrast in this image. Bearing in mind that scanning speed was low enough to disregard statistical fluctuations, sudden intensity variations in the profiles shown in Fig. 2 may be because archaeological ceramic pieces and sherds had been buried for over 1000 years, undergoing weathering and partial removal of the paints, as mentioned above.

5. Conclusions

An image-processing algorithm was developed in MATLAB[®] environment. The program has a user-friendly graphic interface with drop-down menus and the possibility of working with more than one image simultaneously.

The samples analyzed are archaeological ceramic pot sherds from Ambato style of the “Aguada” culture. We have demonstrated that for this kind of samples, the optimization routine complements the analysis accomplished by other techniques.

As corroborated through XRD characterization, the original B53 BSE image presents a mean Z contrast lesser than 0.1. Despite this conventional inconvenience, after an adequate image treatment the discrimination of zones with this low Z contrast was successfully accomplished.

It is necessary to stress out that the methodology presented here can complete the characterization of samples for which X-ray diffraction or X-ray analysis with electron sources is not possible. Backscattered electron images provide information on chemical contrast which cannot be produced with other analytical techniques in a number of particular cases. The ease with which BSE images are acquired for an extended region (a few seconds) encourages further developments in this area since, for example, X-ray imaging is usually a time-consuming procedure (hours) in view of the high noise maps for multicomponent samples—when such a procedure is eventually applicable. In addition, it is clear that image-processing techniques implemented for backscattered electron pictures may well be extended to those cases for which X-ray maps complement the information provided through BSE images. Several developments may be faced, among which the inclusion of frequential filters would be very simple, and would allow the subtraction of periodical fluctuations through Fourier analysis or similar techniques (Bonnet, 2004).

On the other hand, accurate quantitative routines are impossible to perform for a whole region when subtle inhomogeneities are to be evidenced. The methodology proposed here may be useful when the determination of mean atomic numbers for different regions is sufficient for providing relevant information. Such is the case of plagioclase zonation studies, metallic inclusion characterization, monazite dating through U/Th technique, and similar research problems, which will be studied in the next future.

Acknowledgements

This work was financially supported by the FONCYT Agency (project PICT no. 07-17346) and the Secretaría de Ciencia y Técnica (Universidad Nacional de Córdoba) to whom the authors gratefully acknowledge. They are also thankful to Dr. Andrés Laguens and the Museo de Antropología (UNC) for providing ceramic samples from their collection.

References

- Aloupi, E., Karydas, A.G., Paradellis, T., 2000. Pigment analysis of wall paintings and ceramics from Greece and Cyprus. The optimum use of X-ray spectrometry on specific archaeological issues. *X-Ray Spectrom.* 29, 18–24.

- Appolonia, C.R., Espinoza Qui nones, F.R., Arag ao, P.H.A., dos Santos, A.O., da Silva, L.M., Barbieri, P.F., do Nascimento Filho, V.F., Coimbra, M.M., 2001. EDXRF study of Tupi-Guarani archaeological ceramics. *Radiat. Phys. Chem.* 61, 711–712.
- Baldini, M., Carbonari, J., Cieza, G., de Feo, M., del Castillo, M., Figini, A., Rex González, A., Huarte, R., Togo, J., 2002. Primer análisis de la cronología obtenida en el sitio Choya 68 (Depto. de Capayán, Provincia de Catamarca, Argentina). *Estudios Atacame nos* 24, 71–82.
- Bao-Ping, L., Jian-Xin, Z., Greig, A., Collerson, K.D., Zhen-Xi, Z., Yue-Xin, F., 2005. *Nucl. Instr. Meth. Phys. Res. B* 240, 726–732.
- Barrios Neira, J., Montealegre, L., López, L., Romero, L., 2009. Ceramics of Ategua (Córdoba, Spain): mineralogical and petrographic study. *Appl. Clay Sci.* 42, 529–537.
- Bertolino, S.R., Fabra, M., 2003. Provenance and ceramic technology of pot sherds from ancient Andean cultures at the Ambato valley, Argentina. *Appl. Clay Sci.* 24, 21–34.
- Bertolino, S.R., Galván, V., Carreras, A., Laguens, A., De La Fuente, G., Riveros, A., 2009. X-ray techniques applied to surface paintings of ceramic pottery pieces from Aguada Culture (Catamarca, Argentina). *X-Ray Spectrom.* 38, 95–102.
- Bonnet, N., 2004. Some trends in microscope image processing. *Micron* 35, 635–653.
- Bruker AXS, 2004. TOPAS V3.0: General Profile and Structure Analysis Software for Powder Diffraction Data. Bruker AXS, Karlsruhe, Germany.
- Buxeda i Garrigós, J., 1999. Alteration and contamination of archaeological ceramics: the perturbation problem. *J. Archaeol. Sci.* 26, 295–313.
- Cariati, F., Fermo, P., Gilardoni, S., Galli, S., Milazzo, M., 2003. A new approach for archaeological ceramics analysis using total reflection X-ray fluorescence spectrometry. *Spectrochim. Acta Part B: Atom. Spectrosc.* 58, 177–184.
- Chen, S.D., Ramli, A.R., 2003. Minimum mean brightness error by-histogram equalization in contrast enhancement. *Trans. Consumer Electron.* 49, 1310–1319.
- Chinga-Carrasco, G., Lenes, M., Johnsen, P.O., Hult, E.-L., 2009. Computer-assisted scanning electron microscopy of wood pulp fibres: dimensions and spatial distributions in a polypropylene composite. *Micron* 40, 761–768.
- Cochrane, E., Neff, H., 2006. Investigating compositional diversity among Fijian ceramics with laser ablation-inductively coupled plasma-mass spectrometry (LA-ICP-MS): implications for interaction studies on geologically similar islands. *J. Archaeol. Sci.* 33, 378–390.
- Craig, N., Speakman, R., Popelka-Filcoff, R., Glascock, M., Robertson, J., Shackley, M., Aldenderfer, M., 2007. Comparison of XRF and PXRF for analysis of archaeological obsidian from southern Perú. *J. Archaeol. Sci.* 34, 2012–2024.
- De La Fuente, G., Kristcautzky, N., Toselli, G., Riveros, A., 2005. Petrología cerámica comparativa y análisis composicional de las pinturas por MEB-EDS de estilo Aguada Portezuelo (ca. 600–900 DC) en el valle de Catamarca (Noroeste Argentino). *Estudios Atacame nos* 30, 61–78. Available from http://www.scielo.cl/scielo.php?script=sci_arttext&pid=S0718-10432005000200004 (in Spanish).
- De La Fuente, G., 2006. Technological study of pigments and paints on archaeological ceramics from the northwestern Argentine region: an archaeometric approach and implications for conservation. *Glass Ceram. Conserv.* 14, 3–6.
- Dollase, W.A., 1986. Correction of intensities for preferred orientation in powder diffractometry: application of the March model. *J. Appl. Cryst.* 19, 267–272.
- Druc, I., 2001. Introduction. Archaeology and clays. In: Druc, I. (Ed.), *Archaeology and Clays*, British Archaeological Report International Series 942, Oxford, pp. iii–vi.
- Edwards, H.G.M., Chalmers, J.M., 2005. *Raman Spectroscopy in Archaeology and Art History*. Royal Society Of Chemistry, Cambridge.
- Fabra, M., 2006. Estimaciones sobre la inversión artesanal en la producción cerámica (sitio Piedras Blancas, Valle de Ambato, Catamarca). In: Costa, M., Llagostera, A. (Eds.), *IV Round Table La Cultura de la Aguada y su Dispersión*. Inst. Investigaciones Arqueológicas y Museo, Universidad Católica del Norte, San Pedro de Atacama, pp. 7–18.
- Fernández-Ruiz, R., García-Heras, M., 2007. Study of archaeological ceramics by total-reflection X-ray fluorescence spectrometry: semi-quantitative approach. *Spectrochim. Acta Part B: Atom. Spectrosc.* 62, 1123–1129.
- Fortina, C., Memmi Turbanti, I., Grassi, F., 2008. Glazed ceramic manufacturing in Southern Tuscany (Italy): evidence of technological continuity throughout the medieval period (10th–14th centuries). *Archaeometry* 50, 30–47.
- Goldstein, J., Newbury, D., Echlin, P., Joy, D., Romig, A., Lyman, C., Fiori, C., Lifshin, E., 1992. *Scanning Electron Microscopy and X-Ray Microanalysis: A Text for Biologists, Materials Scientists, and Geologists*. Plenum Press, New York.
- Gonzalez, R., Woods, R., 2002. *Digital Image Processing*, 2nd ed. Prentice-Hall, New Jersey.
- Habicht-Mauché, J., Glenn, S.T., Milford, H., Flegal, A.R., 2002. Stable lead isotope analysis of Rio Grande glaze paints and ores using ICP-MS: a comparison of acid dissolution and laser ablation techniques. *J. Arch. Sci.* 29, 1043–1053.
- Inorganic Crystal Structure Database (ICSD) program. Available at <http://icsd.fiz-karlsruhe.de/icsd>.
- Iordanidis, A., García-Guines, J., Karamitrou-Mentessidi, G., 2009. Analytical study of ancient pottery from the archaeological site of Aiani, northern Greece. *Mater. Charact.* 60, 292–302.
- Jafar, I., Ying, H., 2008. New algorithms for contrast enhancement in gray-scale images based on the variational definition of histogram equalization. *Integr. Comput.-Aid. Eng.* 15, 131–147.
- Laguens, A., Juez, M., 1999. Especialización en la manufactura cerámica de pucos Aguada. *Actas del XIII Congreso Nacional de Arqueología Argentina, Córdoba*, vol. II 489–504.
- Laguens, A., Bonnin, M., 2005. Recursos materiales y desigualdad social en la arqueología de Ambato, Catamarca. In: *La Cultura de la Aguada y sus expresiones regionales*. Universidad Nacional de La Rioja, La Rioja, pp. 23–34.
- March, A., 1932. Mathematische Theorie der Regelung nach der Korngestalt bei affiner Deformation. *Z. Kristallogr.* 81, 285–297.
- Mirti, P., 2000. X-ray microanalysis discloses the secrets of ancient Greek and Roman potters. *X-Ray Spectrom.* 29, 63–72.
- Molera, J., Pradell, T., Vendrell-Saz, M., 1998. The colours of Ca-rich ceramic pastes: origin and characterization. *Appl. Clay Sci.* 13, 187–202.
- Neff, H., 2003. Analysis of Mesoamerican plumbate pottery surfaces by laser ablation-inductively coupled plasma-mass spectrometry (LA-ICP-MS). *J. Arch. Sci.* 30, 21–35.
- Neycenssac, F., 1993. Contrast enhancement using the Laplacian-of-a-Gaussian filter. *Graph. Models Image Process.* 55, 447–463.
- Odell, H., 2006. *Lithic Analysis*, 3rd ed. Springer, New York.
- Pantorrilla, M., Núñez Regueiro, V., 2006. Investigaciones arqueológicas en la zona de Escaba, provincia de Tucumán: asentamientos Condorhuasi y Aguada en las Yungas. *Intersecciones en Antropología* 7, 235–245.
- Papadopoulou, D.N., Zachariadis, G.A., Anthemidis, A.N., Tsirliganis, N.C., Stratis, J.A., 2004. Comparison of a portable micro-X-ray fluorescence spectrometry with inductively coupled plasma atomic emission spectrometry for the ancient ceramics analysis. *Spectrochim. Acta Part B: Atom. Spectrosc.* 59, 1877–1884.
- Pérez-Arantegui, J., Resano, M., García-Ruiz, E., Vanhaecke, F., Roldán, C., Ferrero, J., Coll, J., 2008. Characterization of cobalt pigments found in traditional Valencian ceramics by means of laser ablation-inductively coupled plasma mass spectrometry and portable X-ray fluorescence spectrometry. *Talanta* 74, 1271–1280.
- Polak, M., Baram, J., Pelleg, J., 1983. Auger electron spectroscopy applied to the analysis of archaeological artifacts. *Archaeometry* 25, 59–67.
- Reed, S., 1993. *Electron Probe Microanalysis*, 2nd ed. Cambridge University Press, Cambridge.
- Russ, J.C., 1998. *The Image Processing Handbook*, 3rd ed. CRC Press, Boca Raton.
- Sánchez Ramos, S., Bosch Reig, F., Gimeno Adelantado, J.V., Yusá Marco, D.J., Doménech Carbó, A., 2002. Study and dating of medieval ceramic tiles by analysis of enamels with atomic absorption spectroscopy, X-ray fluorescence and electron probe microanalysis. *Spectrochim. Acta Part B: Atom. Spectrosc.* 57, 689–700.
- Savitzky, A., Golay, M.J.E., 1964. Smoothing and differentiation of data by simplified least squares procedures. *Anal. Chem.* 36, 1627–1639.
- Schleicher, L., Miller, J., Watkins-Kenney, S., Carnes-McNaughton, L., Wilde-Ramsing, M., 2008. Non-destructive chemical characterization of ceramic sherds from Shipwreck 31CR314 and Brunswick Town, North Carolina. *J. Archaeol. Sci.* 35, 2824–2838.
- Schreiner, M., Frühmann, B., Jembrih-Simbürger, D., Linke, R., 2004. X-rays in art and archaeology—an overview. *Adv. X-Ray Anal.* 47, 1–17.
- Smith, G.D., Clark, R.J.H., 2004. Raman microscopy in archaeological science. *J. Archaeol. Sci.* 31, 1137–1160.
- Speakman, R.J., Neff, H., 2002. Evaluation of painted pottery from the Mesa Verde region using laser ablation-inductively coupled-mass spectrometry (LA-ICP-MS). *Am. Antiq.* 67, 137–144.
- Tzaphlidou, M., 2005. The role of collagen in bone structure: an image processing approach. *Micron* 36, 593–601.
- Vaughn, K.J., Conlee, C.A., Neff, H., Schreiber, K., 2006. Ceramic production in ancient Nasca: provenance analysis of pottery from the Early Nasca and Tiza cultures through INAA. *J. Archaeol. Sci.* 33, 681–689.
- Young, R., 1993. *The Rietveld Method*. International Union of Crystallography, Oxford University Press, Oxford.